Applied Physics B manuscript No.
(will be inserted by the editor)

Theory of atomic diffraction from evanescent waves

Carsten Henkel[1], Hartmut Wallis[2], Nathalie Westbrook[3], Chris I. Westbrook[3], Alain Aspect[3], Klaus Sengstock[4], Wolfgang Ertmer[4]

[1] Institut für Physik, Am Neuen Palais 10, Universität Potsdam, D–14469 Potsdam, Germany, e-mail: Carsten.Henkel@quantum.physik.uni-potsdam.de
[2] Max-Planck-Institut für Quantenoptik, Hans-Kopfermann-Straße 1, D–85748 Garching, Germany and Sektion Physik, Ludwig-Maximilians-Universität München, Theresienstraße 37, D–80333 München, Germany
[3] Laboratoire Charles Fabry de l'Institut d'Optique, Unité de Recherche Associée au CNRS, B. P. 147, F–91403 Orsay CEDEX, France
[4] Institut für Quantenoptik, Universität Hannover, Welfengarten 1, D–30167 Hannover, Germany (formerly Institut für Angewandte Physik der Universität Bonn, Bonn, Germany)

submitted 29 May 1998

Abstract We review recent theoretical models and experiments dealing with the diffraction of neutral atoms by a reflection grating, formed by a standing evanescent wave. We analyze diffraction mechanisms proposed for normal and grazing incidence, point out their scopes and confront the theory with experiment.

PACS: 32.80.Lg Mechanical effects of light on atoms – 42.25.Fx Diffraction and scattering – 03.75.Dg Atom interferometry

1 Introduction

An evanescent wave is the light field formed in vacuum above a dielectric when a light beam undergoes total internal reflection at the vacuum–dielectric interface. The evanescent wave propagates parallel to the interface and decreases exponentially with distance from the interface, at a scale sligthly smaller than the optical wavelength. In 1982, Cook and Hill [1] proposed using this spatially inhomogeneous light field to construct a repulsive optical potential able to reflect neutral atoms with normal velocities (perpendicular to the interface) of several cm/s. In 1989, Hajnal and Opat [2] proposed to combine two counterpropagating evanescent waves, creating a mirror with a spatially periodic modulation in order to realize a reflection grating (cf. figure 1). At grazing incidence, the diffraction angles are greatly enhanced similar to X ray diffraction from optical gratings, and one obtains a beamsplitter useful for atom optics [3,4] and interferometry [5].

It took several years of theoretical and experimental work [6,7] before efficient diffraction from a stationary evanescent wave was observed [8–10]. This is due, on the one hand, to the experimental difficulties: the diffraction angles are only in the mrad regime because of the small atomic wavelength compared to the grating period; the grating has to achieve both reflection and diffraction of the atomic beam; at grazing incidence, the coupling between the diffraction orders is reduced due to the Doppler effect. Diffraction was first achieved experimentally when all these were overcome: in 1993, in the experiment at Bonn university (Germany), the atomic beam had been slowed down [8], while in 1996, the group at Paris-Nord university (Villetaneuse, France) tilted the beam with respect to the evanescent wave's propagation direction [9]. At normal incidence, the ENS group (Paris, France) reported diffraction in the time domain (1994) [11], and in 1996, the group at the Orsay Institut d'Optique (France) observed that the evanescent wave yields a nonspecular (diffuse) reflection [12], washing out the diffraction peaks, unless in 1997 dielectric surfaces with high surface quality were used [10].

On the other hand, the theory of the atomic reflection grating encountered a number of difficulties: for instance, the atomic motion is very different from a transmission grating because the atoms are also reflected from the grating, excluding the elimination of one direction of motion in the Raman–Nath approximation. In 1992, the group at Bonn university solved the Schrödinger equation for a two-level atom in a coupled-wave formalism [13] and showed that atomic diffraction is possible if

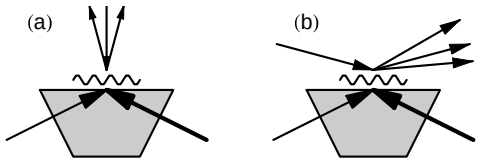

Fig. 1 Schematical setup of an evanescent wave reflection grating. (a): normal incidence, (b): grazing incidence.

the Doppler shift is comparable to both the optical potential and the detuning. The proposed diffraction process involves a delicate interplay of adiabatically followed dressed states and nonadiabatic transitions between them. This approach has been used to interpret numerical calculations [14–16] and allowed a quantitative understanding of experiments on Doppleron resonances [7].

For the case of normal incidence and large detunings, the group at Institut d'Optique (Orsay, France) developed in 1994 an alternative theory based on scalar diffraction, similar to light diffraction from thin phase objects [17,18]. This approach showed that the atomic wave is very sensitive to spatial modulations of the evanescent wave because of its small wavelength, in agreement with the Orsay experiments at normal incidence [10,12]. At grazing incidence however, the same theory predicts vanishing diffraction, in contrast to experiment and the two-level theory [13].

In 1995 the Canberra theory group realized [16] that a numerical integration of the coupled wave equations for a two-level atom at grazing incidence does not reproduce the Bonn experiment [8], indicating that Doppleron resonances do not provide the relevant diffraction mechanism. Since 1996, Gordon and Savage [19], Henkel et al. [20] and Deutschmann [21] pointed out that the observed diffraction at grazing incidence can only be explained in terms of Raman transitions between Zeeman sublevels of the atomic ground state. A similar mechanism had been studied in 1993 by the Bonn group [22] in view of building a grazing incidence beamsplitter from a running evanescent wave and a static magnetic field.

The present paper aims to develop a unified picture of these different theoretical approaches: we review the diffraction mechanisms mentioned above and compare them to each other and to the diffraction experiments reported so far [8–10]. We start in Sec.2 from the most simple description in terms of a 'one-level' optical potential and discuss the results of a perturbative calculation for the diffraction pattern. For normal incidence diffraction, this theory has been extended using semiclassical techniques to compute higher-order diffraction peaks. We then pay particular attention to the case of grazing incidence. In Sec.3, the two-level model of Deutschmann et al. is reviewed. We compare it to the one-level model and give an interpretation why these models make different predictions for the diffraction probabilities. We then apply the two-level model to the diffraction experiments and give an analytical estimate of the Doppleron coupling, showing it to be too small to account for the observed diffraction patterns. On the other hand, the situation is quite different for Raman couplings, as we discuss finally in Sec.4. A simple condition for the optimum diffraction efficiency is derived and we outline some perspectives for experiments with spin-polarized atoms.

2 Diffraction of one-level atoms

2.1 Optical potential

In coherent atom optics, one frequently works in conditions where the atom is driven non resonantly and at low saturation, in order to avoid spontaneous emission processes. Under these circumstances, the theoretical description of the atom–laser-interaction simplifies because the excited state may be eliminated adiabatically. The atomic dynamics is governed by a Schrödinger equation for the ground state wavefunction only ('one-level-atom'), where the light field enters via the so-called 'optical potential' or dipole potential

$$V_{\mathrm{opt}}(\mathbf{r}) = \frac{d^2}{\hbar\delta}|\mathbf{E}(\mathbf{r})|^2 \tag{1}$$

In this expression, d is the reduced matrix element of the atomic dipole operator, $\delta = \omega_L - \omega_A$ is the laser detuning, ω_L (ω_A) is the laser (atomic resonance) frequency, respectively, and $\mathbf{E}(\mathbf{r})e^{-i\omega_L t}$ + c.c. is the laser field.

To begin with, we consider only a single state in the atomic ground state. The atomic wavefunction $\psi(\mathbf{r},t)$ and the Schrödinger equation then become scalar quantities (without Zeeman sublevel indices)

$$i\hbar\partial_t\psi = -\frac{\hbar^2}{2M}\nabla^2\psi + V_{\mathrm{opt}}(\mathbf{r})\psi \tag{2}$$

The AC-Stark-shift has now acquired the meaning of a ponderomotive potential for the center-of-mass motion of atoms without internal structure. Such an approach has found widespread use in theoretical investigations of scalar atom optics, e.g. for the study of *transmission gratings* (see [4] for further references). Although this approach is historically not the first for the reflection grating [the first investigations [2,13] were done for a two-level atom at arbitrary saturation, see Sec.3], it gives the most intuitive understanding of the problem. Its most straightforward application is the description of *'thin'* optical elements, i.e. elements which are characterized by the dynamical phase the atoms accumulate when passing the optical element. Moreover, it allows one to develop far-reaching analytical methods and results that prove useful in the interpretation of more complicated, even non-scalar models.

2.2 Kinematics

2.2.1 Reflection grating. In contrast to a usual transmission grating the atomic reflection grating has to achieve two functions, diffraction and reflection, by a suitably shaped optical potential. A reflective optical potential with a sharp intensity variation along one direction and a periodic intensity modulation along the perpendicular direction, that does this job, can be realized by overlapping two evanescent waves with wavevectors $Q\mathbf{e}_x$ and $-Q\mathbf{e}_x$ parallel to the dielectric surface

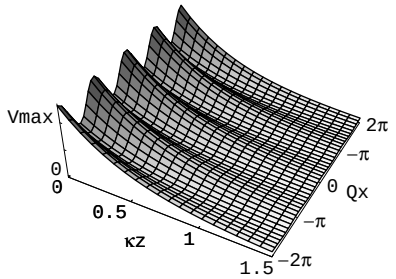

Fig. 2 Optical potential (3) of a partially stationary evanescent wave (contrast $\epsilon = 0.3$).

($Q > k \equiv \omega_L/c$). Denoting the corresponding field amplitudes by $\mathbf{E}_\pm(\mathbf{r}) = \mathbf{E}_\pm \exp(\pm iQx - \kappa z)$, the optical potential (1) becomes

$$V_{\rm opt}(x,z) = V_{\rm max}(1 + \epsilon\cos 2Qx)e^{-2\kappa z} \tag{3}$$

with

$$V_{\rm max} = \frac{d^2}{\hbar\delta}(|\mathbf{E}_+|^2 + |\mathbf{E}_-|^2) \tag{4}$$

$$\epsilon = \frac{2{\rm Re}\,\mathbf{E}_+^* \cdot \mathbf{E}_-}{|\mathbf{E}_+|^2 + |\mathbf{E}_-|^2} \tag{5}$$

The overall height of the potential is given by $V_{\rm max}$, while the dimensionless quantity ϵ determines the *contrast* of the stationary wave. The potential (3) is plotted in Fig.2. The period of the optical potential is equal to $\pi/Q = \lambda/(2n\sin\theta_i)$ and typically a fraction of the optical wavelength (n: index of refraction of the dielectric). The same is true for the decay length $1/2\kappa = \lambda/[4\pi(n^2\sin^2\theta_i - 1)^{1/2}]$.

Atoms impinging on this optical potential will experience a reflection of the z-component of their momentum if their kinetic energy in this direction does not exceed the potential height and they can pick up momentum changes $\pm 2Q$ from the periodic modulation.

In Eq.(3), we have neglected the (typically gaussian) intensity profile of the evanescent wave, assuming plane waves incident inside the dielectric. The present picture also neglects the van der Waals interaction between the atom and the dielectric [23]. This interaction is attractive and becomes larger than the optical potential for distances smaller than roughly $\lambda/4\pi$. The full potential is well approximated by the optical potential (3) for distances larger than this value.

2.2.2 Diffraction channels. We now introduce the diffraction channels for an atom incident from infinity onto the stationary evanescent wave. From energy and momentum conservation for the asymptotic states (at large distance $z \to \infty$ from the grating), one finds that the diffracted matter waves are characterized by the following wavevectors

$$k_{xn} = k_{xi} + 2nQ, \quad n = 0, \pm 1, \pm 2, \ldots \tag{6}$$

$$k_{yn} = k_{yi} \tag{7}$$

$$k_{zn} = \sqrt{k_{zi}^2 - 4nQ(k_{xi} + nQ)} \tag{8}$$

where the incident wavevector equals $(k_{xi}, k_{yi}, -k_{zi})$. In the direction parallel to the grating (the x-direction), the atomic wavevector changes by an integer multiple of the 'grating vector' $2Q$. By translation invariance, the y component is conserved. Finally, the normal (or z-) component is obtained from energy conservation, the optical potential being time-independent. These wavevector transfers may also be understood in the photon picture: in the diffraction process, the atom absorbs a photon from one travelling evanescent wave and emits a (stimulated) photon into the other wave, thereby returning to the ground state. This can be repeated n times for the nth diffraction order. The momentum exchange during the process leads to Eqs.(6, 7). Energy is conserved [Eq.(8)], corresponding to an elastic scattering process, because the two light waves have the same photon energy (frequency).

From Eqs.(6–8), the diffraction angles (with respect to the surface normal) are easily obtained through $\tan\theta_n = k_{xn}/k_{zn}$. In this article, we focus throughout on two limiting cases: normal and grazing incidence. At normal incidence and under typical experimental conditions, the first term in the square root in Eq.(8) dominates the two others: the atoms being incident with a velocity much larger than the recoil velocity $\hbar k/M$, their incident wavevector k_{zi} is much larger than the optical wavevector $k \sim Q$. As a consequence, the normal component of the atomic wave vector changes negligibly, and the diffraction angles are small (of order $\theta_n \simeq 2nQ/k_{zi}$). The diffracted beams have a transverse velocity of the order of a few recoil velocities.

At grazing incidence, the second term in the square root, $-4nQk_{xi}$, is comparable to the first, and diffraction leads to a substantial change of the normal wave vector component. The diffraction angles are hence comparable to the angle of incidence, and the diffraction orders are conveniently separated in space even for a quite fast atomic beam. This enormous enhancement of the diffraction angles represents the main motivation for atomic diffraction at grazing incidence.

Note that the above effect may be interpreted in an alternative way in the reference frame co-moving with the atomic beam. In this frame, the frequencies of the two evanescent waves differ by twice the Doppler shift $\delta_D = Qv_{xi} = \hbar Qk_{xi}/M$, and diffraction is accompanied by an energy transfer $2n\hbar\delta_D$. With this reasoning, one also finds Eq.(8), up to the 'recoil shift' term $4n^2Q^2$ in the root (usually a small correction compared to the first and second terms).

2.3 Diffraction intensities: Born approximation

2.3.1 Diffraction amplitudes. Up to now, we have only specified the kinematics of the diffraction process. In this subsection, we present a first approach to calculate the *diffraction pattern*, i.e. the fraction of atoms

diffracted into the different orders. To this end, we introduce the asympotic form of the atomic wavefunction in the region of vanishing potential (a time-dependent factor $\exp(-iEt/\hbar)$ has been separated)

$$z \to +\infty : \qquad (9)$$
$$\psi(x,z) = \exp i(k_{xi}x - k_{zi}z) + \sum_n a_n \exp i(k_{xn}x + k_{zn}z)$$

The first term represents the incident wave and the sum the diffracted waves. The coefficients a_n are the *diffraction amplitudes* that are related to the diffraction probabilities π_n according to

$$\pi_n = |a_n|^2 \frac{\mathrm{Re}\, k_{zn}}{k_{zi}} \qquad (10)$$

[Diffraction orders with imaginary k_{zn} are evanescent. They are localized in the optical potential and do not contribute to the wavefunction at infinity.]

To calculate the diffraction amplitudes a_n, one has, in principle, to solve the stationary Schrödinger equation subject to the asymptotic condition (9), expand the wavefunction in the region $z \to +\infty$ into a Fourier series with respect to x and read off the expansion coefficients. This is a difficult task that may only be accomplished numerically, using e.g. a coupled-wave expansion (see Sec.3.2 and Refs.[13–16]). An additional complication arises from the fact that the atoms are not only diffracted, but also reflected from the optical potential. This translates into a second asymptotic condition, namely that the wavefunction matches an exponentially decreasing solution inside the potential. [Corrections to this picture due to tunneling through the optical potential towards the dielectric are discussed in [24].] For the same reason, we cannot use Fermi's Golden Rule to compute the diffraction amplitudes because in this formula, initial and final states are approximated by the corresponding asymptotic states (the plane waves of Eq.(9)) that are, however, a very bad approximation to the true wavefunction deep inside the potential.

2.3.2 Distorted-wave Born approximation. The way to circumvent this problem and to obtain analytical results for the diffraction amplitudes dates back to the 1930's [25] when Lennard-Jones and Devonshire calculated the diffraction of a thermal atomic beam from a periodic (crystalline) surface. The idea is to treat first the unmodulated potential (that provides the momentum transfer for the basic reflection process) in an exact manner, and then to use perturbation theory for the modulated part of the potential. One obtains a modified Fermi's Golden Rule where wavefunctions $\psi_{i,f}(z)$ are used that decrease inside the potential and asymptotically contain an incident and a specularly reflected wave. The matrix element evaluated in the Golden Rule thus reads

$$A_{fi} = \langle \psi_f(z)|\, e^{-2\kappa z}\, |\psi_i(z)\rangle = \int_{-\infty}^{+\infty} \mathrm{d}z\, \psi_f^*(z) e^{-2\kappa z} \psi_i(z) \qquad (11)$$

This approach to the diffraction problem is called the 'distorted wave Born approximation' (DWBA) in the following. It is a perturbative one and of course valid only for a stationary evanescent wave with low contrast such that nonzero diffraction orders are weakly populated.

When the DWBA is applied to the optical potential (3), one notes first that the Schrödinger equation for the flat potential (an exponentially increasing potential barrier) has an analytical solution [26,27], and second that the matrix element of the modulated part of the potential may be evaluated in closed form [28,29]. In the present notation, one thus obtains the following result for the diffraction probabilites [neglecting exponentially small corrections of order $\exp(-\pi k_{zi}/\kappa)$]

$$\pi_{\pm 1,\mathrm{DWBA}} = \frac{\epsilon^2}{4} \left(\frac{k_{z,\pm 1} + k_{zi}}{2\kappa} \right)^2 \beta^2[(k_{z,\pm 1} - k_{zi})/\kappa] \qquad (12)$$

where the dimensionless factor $\beta(\xi)$ is defined by

$$\beta(\xi) = \frac{\pi\xi/2}{\sinh(\pi\xi/2)} \qquad (13)$$

and reaches its maximum value (unity) for $\xi = 0$.

Note that the DWBA gives the lowest order contribution to the diffraction pattern. It hence determines only the intensities of the first-order diffraction peaks ($n = \pm 1$). Calculations to second order are possible, though much more involved because one has to integrate over a continuous spectrum of intermediate states.

2.3.3 Physical interpretation.

Diffraction efficiency. We first note that the diffraction process may be quite efficient even for a small contrast ϵ. Indeed, if the factor β in (12) is close to its maximum value, the diffraction peaks have a height proportional to the square of the product $\epsilon k_{zi}/\kappa = 2\pi\epsilon \cos\theta_i/(\kappa\lambda_{\mathrm{dB}})$, and since λ_{dB}, the wavelength of the incident matter wave, is typically much smaller than the decay length $1/\kappa$, the contrast ϵ is multiplied by a large number.

To understand this feature, let us consider the potential of Fig.2. Obviously the contours of the potential equalling a given atomic kinetic energy are nearly sinusoidal curves in the xz plane. This suggests to replace the optical potential of the stationary evanescent wave by an infinitely high wall with a spatially modulated position [the 'corrugated hard wall' potential used in atom-surface scattering theory [30,31]]

$$z(x) = (\epsilon/2\kappa)\cos 2Qx. \qquad (14)$$

The atomic wave acquires a position-dependent phase shift $\delta\phi(x) = 2k_{zi}z(x)$ upon reflection from this barrier. The phase of the outgoing wave hence shows a phase modulation $u\cos 2Qx$ with a modulation depth $u = \epsilon k_{zi}/\kappa$. The phase-modulated wave may be expanded into sidebands, and the intensity of the first-order sidebands is given by (for small contrast)

$$\text{hard wall:} \quad \pi_{\pm 1} \simeq \frac{u^2}{4} = \frac{\epsilon^2}{4}\left(\frac{k_{zi}}{\kappa}\right)^2 \qquad (15)$$

This coincides with Eq.(12) in the regime $k_{z,\pm 1} \approx k_{zi}$ where $\beta \equiv 1$. The intensity of the sidebands is comparable to that of the carrier when the phase modulation depth approaches unity. This means that the amplitude of the hard-wall corrugation, $\epsilon/2\kappa$, must be comparable to the wavelength of the incident wave. The latter being much smaller than the optical wavelength, a low contrast ϵ is sufficient to deeply modulate the atomic phase.

This picture of course ignores the finite width of the optical potential. We show now that this width is related to the behaviour of the factor β in (12) as a function of the *normal wavevector transfer* $\Delta k_{zn} = k_{zn} - k_{zi}$.

Normal vs. grazing incidence. The function $\beta(\Delta k_{zn}/\kappa)$ (13) rapidly vanishes as soon as the normal wavevector transfer Δk_{zn} exceeds the evanescent wave decay constant κ. It is close to its maximum value of 1 near normal incidence where the normal wavevector transfer Δk_{zn} is small and varies quadratically with the grating vector Q [Eq.(8), recall that typically $Q \ll k_{zi}$]. On the contrary, at *grazing* incidence, $\Delta k_{z,\pm 1}$ is much larger than κ and β decreases exponentially fast:

$$|\Delta k_z| \gg \kappa: \quad \beta(\Delta k_z) \simeq \frac{\pi|\Delta k_z|}{\kappa}\exp\left(-\frac{\pi|\Delta k_z|}{2\kappa}\right) \qquad (16)$$

This fact practically induces a cutoff in the diffraction process for momentum transfers $|\Delta k_{zn}| \gg \kappa$. In particular, the DWBA predicts a vanishing diffraction efficiency for one-level atoms at grazing incidence. This feature is in contradiction with the experiments at grazing incidence [8,9], and we would like to discuss it in more detail.

Consider the matrix element A_{fi} (11) that appears in Fermi's Golden Rule when the DWBA is used. The z-integral is in fact limited to a narrow interval of width $1/\kappa$ because in the classically forbidden region $z \to -\infty$, the wavefunctions $\psi_{i,f}(z)$ vanish exponentially whereas in the region $z \to +\infty$, the exponential potential limits the integral. The integrand in Eq.(11) is hence an oscillating function due to the interference between the initial and final waves, with an envelope of width $\sim 1/\kappa$. Applying an argument familiar from the theory of Fourier transforms, we may now estimate that A_{fi} is significantly different from zero only if the difference between the wavevectors k_{zi}, k_{zf} is smaller than the inverse width of the envelope:

$$A_{fi} \neq 0 \quad \Leftrightarrow \quad |k_{zf} - k_{zi}| \leq \kappa \qquad (17)$$

Otherwise stated, the diffraction from a standing evanescent wave only provides a 'photon momentum' of order $\hbar\kappa$ in the normal direction.[1] (For an atomic transmission grating, this was pointed out in 1987 by Martin et al. [32].) The functional form of A_{fi} depends on the envelope of the integrand in the matrix element. Noting that this envelope is a smooth function of position, the general properties of Fourier transforms imply that A_{fi} becomes exponentially small for wavevector transfers much larger than the limit (17); this may also be checked from the exact result (12, 16). This behaviour is in sharp contrast to the hard-wall potential that efficiently provides large wavevector transfers in the normal direction, as seen in the model of the preceding paragraph. In their paper [28], Armand and Manson used the modulated exponential potential in order to study the impact of a finite-width interaction potential in atom–surface scattering, in comparison to the corrugated hard wall model. They also observed that diffraction decreases if the potential gets 'softer'.

We are hence led to the conclusion that in the framework of the present (scalar) model, no atomic diffraction is predicted at grazing incidence, which indicates the need for an alternative approach in order to interpret the experimental results [8,9] obtained in this geometry. This will be done in Secs.3 and 4.

2.4 Diffraction intensities: semiclassical perturbation method

In this paragraph, we continue discussing the case of normal incidence in order to compute higher-order diffraction peaks. In fact, the sensitivity of diffraction to weakly modulated potentials calls for a generalization of the approach discussed so far, to go beyond the first-order calculation of the DWBA. The method we present here was developed by Henkel et al. [17], elaborating on ideas of Cohen-Tannoudji [18]. It still leads to analytical results for the peak intensities and provides a simple physical picture for the diffraction process, substantiating the heuristic approach of the corrugated hard-wall potential introduced above. The main difference to the DWBA is that the new approximation scheme remains valid for much larger values of the contrast ϵ where the diffraction pattern typically contains a large number of peaks. Another important difference to the DWBA is to use right from the start semiclassical concepts like trajectories and phases to compute the diffraction pattern. This approach is justified by the experimental conditions where the atomic wavelengths are generally much

[1] This is not in contradiction with the fact that the reflection reverses the incident momentum, since reflection is due to the flat potential that is treated exactly (to arbitrary order). Diffraction, on the contrary, is caused by the modulated part of the potential that, to lowest order, has to provide the momentum transfer between the diffraction channels.

smaller than the optical wavelength (the typical scale of the diffraction grating).[2]

2.4.1 Outline. It is instructive to recall the example of light diffraction from an acoustic wave with a weak index modulation, as discussed in Ch. 12 of Born and Wolf [35]. After the passage through the acoustic wave, the light field has been phase-modulated, and the diffraction intensities are obtained from a Fourier transform of the field amplitude at the exit of the interaction zone. A simple way to calculate the optical phase modulation is to accumulate the refraction index along straight rays through the acoustic wave. Note that this 'recipe' is less accurate than the geometrical optics approximation since it discards the deflection of the rays due to the index gradient. If this deflection is small, the grating may be called 'thin' and for this reason, the outlined method has been termed the 'thin phase grating approximation' (TPGA). Its results are identical to those obtained in the Raman–Nath-approximation [17,35].

At first sight, the TPGA does not seem to apply to the atomic reflection grating we are interested in, since the 'rays' (classical paths) are substantially distorted even for the simple reflection. We now show that the TPGA may nevertheless be used (see [17,18] for details). The basic idea is to compute, for a weakly modulated diffraction grating, the phase shift of the atomic wave to lowest order in the contrast ϵ. [This approximation does not necessarily imply only first-order diffraction because the diffraction pattern will contain several orders if the resulting phase modulation depth is large.] In this calculation, we may use some basic concepts of Lagrangian classical mechanics. Recall that for a given trajectory linking two points, the atomic phase is equal to the classical action integral S_{cl}, divided by Planck's constant $\hbar$. According to the principle of least action, the classical trajectory that solves the equations of motion corresponds to an extremum (actually a minimum) of the action integral. This property allows us to compute the action S_{cl} without explicitly solving the equations of motion: *we obtain a value for S_{cl} accurate to first order even if the action integral is calculated along a nearby path.* For the evanescent wave diffraction grating with a weakly modulated potential, we thus get the atomic phase modulation from an integral along the classical path reflected at the *flat* (non modulated) optical potential because this path is close to the 'real' path. Using the TPGA in this way, one obtains a simple analytical result because both the classical trajectory in the flat potential and the relevant integral along it are explicitly known [27,36,37], while the real path is more difficult to calculate.

[2] This remark also shows why the DWBA is useful in its own right; namely, it also allows one to study diffraction in the very-low-energy domain where the atomic wavelength is comparable to the scales of the diffraction grating. This regime has not yet been thoroughly explored in experiments, though it should lead to interesting quantum effects [33,34].

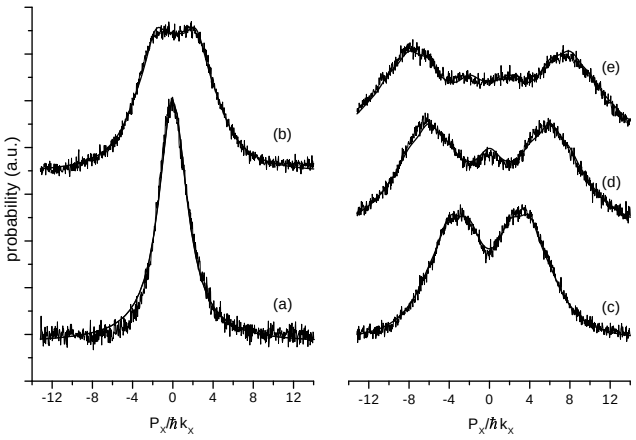

Fig. 3 (courtesy of A. Landragin, Ref.[10]) Atomic momentum distributions after normal-incidence reflection from an evanescent wave with a weak stationary component (intensity ratio of order 10^{-4}). The amplitude of the standing wave increases from (a) to (e). The solid line is a theory based upon the thin phase grating approximation: squared Bessel functions convoluted with the specular reflection pattern (a), the modulation index being the only fit parameter.

The perturbative approach just outlined is called the 'thin phase grating approximation' (TPGA) by analogy to the method used in light diffraction. The atomic diffraction grating is 'thin' if the actual classical paths are only slightly perturbed by the modulated potential. In particular, one has to avoid focal points and caustics inside the interaction region (see [17] for a detailed discussion). We note that in neutral atom scattering from crystalline surfaces, the TPGA is well known under the name 'trajectory approximation' [31,36]. In the field of cold neutron wave optics, similar approaches have been discussed by Felber et al. [38].

2.4.2 Discussion. When the thin phase grating approximation is applied to the atomic diffraction problem, the reflected atomic wave is phase-modulated with an amplitude

$$u_{\mathrm{TPGA}} = \epsilon \frac{k_{zi}}{\kappa} \beta[(2Q/\kappa)\tan\theta_i] \qquad (18)$$

where the cutoff function β defined in Eq.(13) has been used. The diffraction pattern predicted from the TPGA is thus familiar from phase modulation: the diffraction peaks have weights given by the squares $J_n^2(u)$ of Bessel functions (see also Fig.3). In the perturbative regime $u \ll 1$, the pattern consists of a strong 'carrier' (zeroth order peak) plus symmetrical sidebands (diffraction orders $n = \pm 1$) with a weight of order $u^2/4$. In the opposite regime $u \gg 1$, sidebands up to order $n \approx \pm u$ are populated, with a broad maximum at the extreme orders. For a modulation index $u \approx 2$, the orders $n = \pm 1$ are maximized to a height ≈ 35 % each.

In order to establish the validity of the TPGA, let us consider the perturbative regime because there, the DWBA provides us with a 'benchmark result'. At normal incidence, $\theta_i = 0$ and we recover, for a weak phase modulation $u \ll 1$, the result (12) of the DWBA *provided* the normal wavevector difference $\Delta k_{z,\pm 1}$ is small compared to κ. Expanding this difference to second order in Q, we hence find a condition of validity of the thin phase grating method[3]

$$|\Delta k_{z,\pm 1}| \approx \frac{2Q^2}{k_{zi}} \ll \kappa, \tag{19}$$

a condition that is typically satisfied in diffraction experiments. The TPGA hence extends the DWBA result to the regime of large atomic phase modulation. Its predictions agree with diffraction experiments at normal incidence, as illustrated by Fig.3 taken from Ref.[10].

We conclude this paragraph with an alternative interpretation for the cutoff of the diffraction efficiency at grazing incidence, based on an argument given in 1987 by Martin et al. for a transmission grating [40]. In the TPGA, one gets the atomic phase modulation by accumulating the sinusoidal part of the potential during the reflection from the flat potential. At grazing incidence, it happens that the classical path passes through a large number of standing wave periods during the interaction time τ. As a consequence, the standing wave exerts a rapidly oscillating potential that tends to average out. Since this oscillation frequency is given by twice the Doppler shift $2Qv_{xi}$, we may expect the modulation index to be very small in the regime $2Qv_{xi}\tau \gg 1$. Taking an interaction time $\tau = 1/(\kappa v_{zi})$) for the evanescent wave reflection grating, we recover the argument of the cutoff function β in Eq.(18), and the asymptotic expansion (16) confirms our expectation of a vanishing modulation index. This cutoff has been observed in experiments performed in the time domain [11], see also [29, 38], and very recently in spatial diffraction experiments [42]. Balykin et al. proposed a method to restore efficient atomic diffraction at grazing incidence [41]: they reduce the grating vector $2Q$ by using a modulated evanescent wave above a structured surface with a period in the μm range.

3 Diffraction of two-level atoms

The results of the preceding Section suggest that the one-level model cannot explain evanescent wave diffraction at grazing incidence because the 'bandwidth' of this grating is interaction-time limited. In order to understand why experiments at grazing incidence nevertheless showed diffraction, more complex models are needed and have been introduced, in fact, prior to the one-level model discussed so far. These models have in common that they include, to a certain extent, the atomic multilevel structure. Historically the first approach to do so is the extensively used two-level atom [2,13–16,43] that allows an accurate description of the atom-light interaction at any degree of saturation. The 'next generation' also includes the magnetic sublevel structure of the atomic ground state [22,19,20]. We discuss in this Section the two-level diffraction theory developed by Deutschmann et al. [13]. Its relation to the one-level model is analyzed in some detail, since it takes a quite different route to explain the diffraction process.

3.1 General

We focus again on the coherent interaction between a two-level atom and a monochromatic laser field and assume again that spontaneous emission is negligible. The atom is then described by a two-component wavefunction $(\psi_g, \psi_e)^T$ whose evolution is governed by the following (r.w.a.) Hamiltonian matrix

$$H = -\frac{\hbar^2}{2M}\nabla^2 - \begin{pmatrix} 0 & dE^*(\mathbf{r}) \\ dE(\mathbf{r}) & \hbar\delta \end{pmatrix} \tag{20}$$

The notations are identical to Eq.(1), and we recall the electric field amplitude

$$E(\mathbf{r}) = (E_+ \exp iQx + E_- \exp(-iQx))\, e^{-\kappa z}. \tag{21}$$

The laser field couples the ground and excited states, and therefore new diffraction channels open up where the atom leaves the interaction region in the excited state. From momentum conservation, these channels correspond to an odd number of exchanged photon momenta along the x-axis: $k_{x\nu} = k_{xi} + \nu Q$ with $\nu = 2n+1$. For the odd diffraction orders, the detuning δ between the photon energy and the atomic internal energy has to be taken into account since the atoms end up in a different internal state (the scattering is *inelastic*). Using energy conservation, the normal wavevector component is obtained as

$$\nu \text{ odd:} \qquad k_{z\nu} = \sqrt{k_{zi}^2 + 2M\delta/\hbar - \nu Q(2k_{xi} + \nu Q)} \tag{22}$$

For even ν, $k_{z\nu}$ is still given by Eq.(8) with $n = \nu/2$.

[3] Note that the TPGA method does not correctly describe the wavevector transfer normal to the grating. Roughly speaking, this failure is related to the choice of the classical trajectory along which the phase shift is computed. In the context of atomic interferometry, Bordé has presented a generalization of the TPGA that correctly includes the term quadratic in Q (the recoil term) [39]. Similar improvements have also been reported for thermal atom scattering from crystalline surfaces (see [31] for a review).

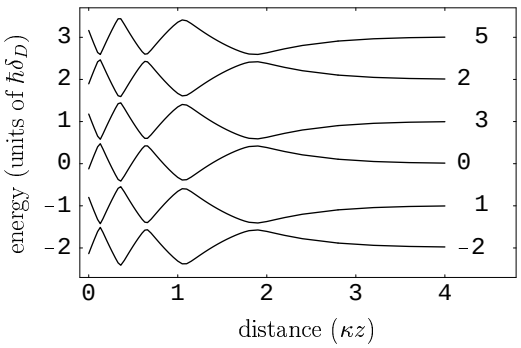

Fig. 4 Adiabatic potentials in a stationary evanescent wave. The potential surfaces are labeled according to the diffraction channels they asymptotically connect to. The detuning is $\delta = 2\,\delta_D$.

3.2 Coupled wave analysis

To solve the Schrödinger equation with the Hamiltonian (20), it is convenient to use a mixed position-momentum representation. This takes advantage of the discrete momentum change along the x-direction, while the dynamics normal to the grating is treated in the position representation. The wavefunctions are thus expanded in Fourier series with respect to the x-coordinate:

$$\psi_g(x,z) = \sum_{\nu\,\mathrm{even}} \psi_\nu(z) \exp ik_{x\nu}x \tag{23}$$

$$\psi_e(x,z) = \sum_{\nu\,\mathrm{odd}} \psi_\nu(z) \exp ik_{x\nu}x \tag{24}$$

In this representation, the coupling term in the Hamiltonian (20) becomes an infinite-dimensional matrix $V_{\nu\mu}$, and the stationary Schrödinger equation takes the following form

$$-\frac{\hbar^2}{2M}\frac{d^2}{dz^2}\psi_\nu + \sum_\mu V_{\nu\mu}(z)\psi_\mu = \frac{\hbar^2 k_{zi}^2}{2M}\psi_\nu \tag{25}$$

A direct numerical solution of these equations is in principle possible and has been performed [2,14,15]. Recently, also some analytical work has been reported on the reflection problem [44].

3.2.1 Adiabatic potentials. In order to simplify the solution and to gain qualitative understanding, Deutschmann et al. diagonalize the coupling matrix $V_{\nu\mu}(z)$ in the coupled-wave equations (25). Its position-dependent eigenvalues $W_\nu(z)$ are called the 'adiabatic' or 'dressed state' potentials, where the latter term draws on the analogy to a two-level atom in a standing laser wave [45]. An example of the adiabatic potential surfaces is given in Fig.4.

One observes in this figure that far from the evanescent wave, the potential surfaces are of two types that are either repulsive or attractive. For each type, the potentials form an asymptotically equidistant series with a separation equal to twice the Doppler shift. [Strictly speaking, the levels are not equidistant due to the 'recoil term' quadratic in Q, but this is typically a small correction at grazing incidence.] For a positive detuning, repulsive potentials connect to the ground state channels discussed above for the 'one-level atom', while attractive potentials asymptotically connect to excited state channels (ν odd). Inside the evanescent wave, we observe that repulsive and attractive potential surfaces approach each other, although without crossing. This is because the ground and excited states are coupled by multiphoton transitions, so-called Doppleron resonances [46]. These 'avoided crossings' play a key role in the diffraction mechanism, as is discussed now.

3.2.2 Diffraction mechanism. Consider a ground state atom that enters the stationary evanescent wave in the channel $\nu = 0$ and follows the potential $W_0(z)$. In order to have diffraction, it has to make a transition to a different potential surface, otherwise it would be reflected in the $\nu = 0$ channel or hit the surface. Such a transition occurs if the atom cannot follow adiabatically the potential surface $W_0(z)$. This is indeed possible because the transformation that diagonalizes the coupling matrix $V_{\nu\mu}(z)$ depends on the position z and does not commute with the kinetic energy operator in the Schrödinger Eq.(25). The dressed levels thus become *nonadiabatically coupled.* In order to compute the nonadiabatic transitions between the adiabatic potentials, Deutschmann et al. exploit the circumstance that nonadiabatic couplings are only important between levels that are 'close' in energy. As can be seen from Fig.4, this implies that the couplings are spatially localized around avoided crossings of the adiabatic potentials. In their vicinity, one may make a two-state approximation and use a generalization of the Landau-Zener formula to compute the wavefunction amplitudes in the two dressed states after the atom has passed the avoided crossing (see [13] for details).[4]

We are thus led to the following picture for the diffraction process: the incoming atomic wave propagates through the dressed levels and is split and recombined in the avoided crossings. This creates a number of partial waves that propagate either towards the dielectric surface or escape into vacuum, after having been reflected from a repulsive potential. The stationary evanescent wave is hence physically equivalent to an array of beamsplitters (avoided crossings) and mirrors (repulsive potentials), and the diffraction pattern is determined from the beamsplitters' efficiencies and the

[4] The picture presented so far is only accurate in a semiclassical regime where a generalized Landau-Zener theory for the avoided crossings applies. It becomes questionable for atoms with a low kinetic energy because of wave-mechanical effects. In this regime, Deutschmann et al. numerically solved a multi-component Schrödinger equation with appropriate boundary conditions.

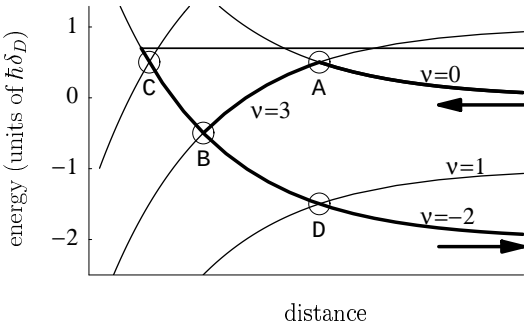

Fig. 5 Typical path of an atom through the adiabatic potentials that leads to diffraction into the $\nu = -2$ ground state channel. The four circles mark avoided crossings. The optimized detuning is chosen: $\delta = 2\,\delta_D$.

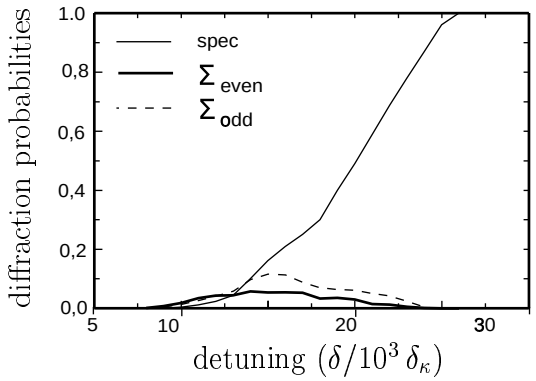

Fig. 6 (courtesy of R. Deutschmann, Ref.[13, 21]) Predictions of the two-level model for the populations as a function of the laser detuning (in units of the 'recoil frequency' $\delta_\kappa \equiv \hbar\kappa^2/2M$).Thin solid curve: specular ($\nu = 0$) order; thick solid curve: even nonzero orders; dashed curce: odd orders. The Doppler shift is taken equal to $\delta_D = 6.52 \times 10^3\,\delta_\kappa$. For a detuning $\delta = 2\delta_D$, the even diffraction orders $\nu = \pm 2$ are maximized to a total population of about 6 %. The Stueckelberg oscillations are averaged over by convolution with a finite energy width for the incoming atoms.

'optical path lengths' between the splitters and mirrors. The atoms traverse this array much like balls on a Galton board with the difference that all the different paths are in principle taken at the same time, their amplitudes having to be added to obtain the amplitude for diffraction into a given order.

The performance of the reflection grating is limited by the fact that the evanescent wave has to achieve both diffraction and reflection of the wavefunction. These tasks are actually incompatible: for vanishing modulation $\epsilon = 0$ (single running evanescent wave), the ground state potentials are repulsive, yet there are no avoided crossings with attractive potentials. For maximum modulation $\epsilon = 1$ (a pure standing wave) on the other hand, strong avoided crossings lead to adiabatic potentials widely separated in energy and essentially flat; the incoming atoms traverse the evanescent field and hit the surface. The most efficient operation of the diffraction grating is obtained for an intermediate contrast. Another important condition is to achieve an optical potential comparable to the Doppler shift: this assures that the potential surfaces for the ground and excited states actually cross. The available laser power being limited, one has to reduce the Doppler shift Qv_{xi} to meet this condition [8,9]. At optimized operation, the diffraction probabilities are still small, however: recall that in an avoided crossing, the atom makes a transition to an adiabatic potential of excited state character. In order to end up finally in a ground state diffraction channel, it must pass several crossings. Deutschmann et al. argue that at least four crossings are involved, as shown schematically in Fig.5. Since one of these beamsplitters (marked B) is passed twice, first in reflection and second in transmission, it is optimized with a 50 : 50 splitting ratio. Assuming a perfect reflection at the innermost crossing (C) and a similar splitting ratio for the two outer crossings (A, D), one is led to a diffraction probability of the order of $(1/2)^4 \simeq 6$ % for the $\nu = -2$ ground state channel. This value is indeed typical for the results obtained in numerical calculations [13], as shown in Fig.6. Diffraction being optimized, the specular population ($\nu = 0$ channel) is only around 20 % because in a number of crossings, the atoms are transmitted to the prism surface and lost. The predicted diffraction probabilities also contain delicate oscillating features, so-called Stueckelberg oscillations, that are due to interferences between different paths through the potential surfaces (not shown in Fig.6).

3.3 Comparison to one-level model

The picture developed by Deutschmann et al. seems so largely different from the one-level atom that a comparison of the two models is desirable.

First, *why do these models make different predictions for atomic diffraction at grazing incidence?* We have seen that in the two-level model, the diffraction mechanism crucially depends on a resonant coupling to the excited state playing the role of an intermediate state for diffraction into a ground state channel. It is obvious that the one-level model *cannot reproduce* this resonant mechanism, since it eliminates the excited state right from the start, assuming it to be off-resonant.

While this answers the first question, it leads us to a second one concerning normal incidence: *how can we interpret the efficiency of diffraction at normal incidence in the adiabatic potential picture?* At normal incidence, the Doppler shift is very small, and the adiabatic potentials are hence quite close (with a separation of the order of the recoil energy). A simple estimation shows that for typical atomic velocities, there are strong nonadia-

batic couplings between the dressed states, *even outside* avoided crossings [47]. The atomic wavefunction is coupled to other diffraction channels all over the evanescent wave, and the idea of spatially localized beamsplitters, that is used in the scheme set up by Deutschmann et al., fails in this regime. By contrast the one-level model does take into account such a spatially extended coupling. In the thin phase grating approximation, e.g., this is done by accumulating the phase due to the modulated evanescent wave potential (that provides the coupling) along the path the atom follows during reflection.

Note finally that the preceding argument also allows one to interpret *why the diffraction efficiency is cut off at grazing incidence in the scalar model*: with increasing Doppler shift, the adiabatic potentials for ground-state diffraction channels become more and more separated, and the probability of nonadiabatic transitions decreases exponentially with the level separation [Kazantsev et al. discussed a similar result in 1980 for two-level atoms and a transmission grating [48]]. The atom hence stays adiabatically in its initial repulsive dressed level, and no transitions to other (ground state) diffraction channels take place.

3.4 Comparison to experiment

We have to distinguish between two regimes depending on the value of the detuning compared to the Doppler shift.

The two-level model predicts optimized diffraction for a detuning $\delta = 2\,\delta_D$ (see Fig.6). Ground and excited states are then efficiently coupled by a low-order Doppleron resonance. Recall that in this resonance, the atom absorbs a number $l+1$ of photons from one running evanescent wave and emits l photons into the other, counterpropagating, wave. The resonance condition for this process depends on the Doppler shift and reads $\delta = (2l+1)\delta_D$ in weak fields [46]; it is shifted towards smaller detunings in the presence of light-shift potentials [7]. Optimum diffraction is mediated by a three-photon Doppleron (the avoided crossing between the channels $\nu = 0, 3$ in Fig.4) whose 'effective Rabi frequency' is comparable to the optical potential. Once the atom has been excited, however, it is subject to an attractive optical potential and likely to hit the dielectric surface and be lost from the incident beam. As discussed above, this is the dominant process for a pure standing wave where the adiabatic potentials are widely split at avoided crossings. The two-level model is thus able to describe the Doppleron resonance experiments of the Paris-Nord (Villetaneuse) group [49] and of the Canberra group [7] where the evanescent wave's reflectivity was measured as a function of detuning.

If the detuning is much larger than the Doppler shift, the two-level model predicts a vanishing diffraction efficiency (see Fig.6). This regime corresponds however to the diffraction experiments in Bonn [8] and in Paris-Nord (Villetaneuse) [9]. There, an atomic beam was split upon reflection from a partially stationary evanescent wave. Both groups checked that the angle of the secondary beam was in accordance with the kinematics of a diffraction process. While the Bonn group observed an efficiency of a few percent, in apparent agreement with the two-level theory, the Villetaneuse group reported a splitting of up to $60:40$ for the $\nu = 0, -2$ channels. It is impossible to explain these experiments with the two-level theory because for a detuning δ much larger than the Doppler shift, the Doppleron resonances yield a negligible diffraction efficiency. This was observed numerically by Gordon and Savage [19] and by Deutschmann [21], and we would like to give here an analytical estimate for the Doppleron coupling.

For the experimental parameters of the diffraction experiments [8,9], the relevant Dopplerons involve a large number of photons ($2l+1$ between 10 and 20). In this regime, eliminating the $2l$ intermediate states, one finds an 'effective Rabi frequency' of order [47,50, 51]

$$\hbar\Omega_{\mathrm{eff}} \simeq V_0(z_c)\left(\frac{dEe^{1-\kappa z_c}}{\hbar\delta}\right)^{2l-1} \ll V_0(z_c) \qquad (26)$$

where z_c is the position of the avoided crossing. This Rabi frequency is negligible compared to the optical potential $V_0(z_c)$ for a detuning δ larger than the one-photon Rabi frequency $dEe^{-\kappa z_c}/\hbar$. In the adiabatic potential picture, the avoided crossing becomes a nearly perfect crossing, and the atom follows its repulsive potential as if the attractive potential did not exist. The 'beamsplitter' is thus perfectly 'transparent', no splitting and hence no diffraction occur.

3.5 Summary

The diffraction of two-level atoms at grazing incidence is possible if the atom makes a sequence of transitions that involve, at an intermediate stage, dressed states of excited character. This mechanism is effective at low detunings where Doppleron resonances provide an efficient coupling. For a pure standing evanescent wave, it leads to a reduced number of reflected atoms because the excited state is transmitted down to the dielectric surface. At the large detunings typical for grazing incidence diffraction experiments, however, Doppleron resonances become negligible, and these experiments call for another model. This has been realized by the Bonn group who published, shortly after the two-level theory, a proposal for an atomic beamsplitter that involves transitions between ground state Zeeman sublevels [22,21]. The Canberra theory group noticed that Zeeman sublevels are necessary for evanescent wave diffraction when they observed that a numerical integration of the coupled-wave equations (25) gave negligible diffraction for the parameters used in the experiment [16,19].

4 Model with multiple ground state sublevels

We now review the diffraction theories that take into account the Zeeman (magnetic) degeneracy of the atomic ground state. We first outline the corresponding mechanism and then summarize the theoretical work done so far.

4.1 General

Atomic diffraction occurs when the atom absorbs a photon from one running evanescent wave and emits one into the other counterpropagating wave. This 'Raman transition' corresponds to a momentum transfer and leads to the splitting of the atomic beam in momentum space. At grazing incidence, the running evanescent waves that form the diffraction grating acquire a frequency difference in the frame of the atomic beam that equals twice the Doppler shift. If the Raman coupling connects the same ground state sublevel, it is hence far off resonance and no efficient population transfer may take place. But the Raman transition may also connect different Zeeman sublevels and become resonant if the sublevel degeneracy is lifted. This happens, e.g., in a static magnetic field (Zeeman effect) or in a suitably polarized light field. The first scenario has been explored for a running evanescent wave by Deutschmann et al. [22], in view of building an atomic beamsplitter. In the context of the evanescent wave diffraction grating, the second scenario was studied numerically in the Canberra theory group [19] and analytically in the Orsay group [20].

4.2 Physical picture

For a basic understanding of the diffraction mechanism, let us consider the limit of low saturation and a detuning large compared to both the Doppler shift and the natural linewidth. The excited state manifold may then be eliminated adiabatically, and for a ground state of angular momentum J_g, the atomic wavefunction is described by the $2J_g+1$ components $\psi_m(x,z)$, $m=-J_g,\ldots+J_g$. It is subject to an optical potential $\hat{V}(z)$ whose matrix elements are of the form [we suppose that Doppler shift δ_D and Zeeman shift are negligible compared to the detuning δ]

$$\langle m|\,\hat{V}(z)\,|m'\rangle = \frac{d^2}{\hbar\delta}\sum_{q,q',m_e} E_q^*(\mathbf{r})E_{q'}(\mathbf{r})\times \\ \times\,(J_g,m;1,q|\,J_e,m_e)\,(J_e,m_e|\,J_g,m';1,q') \quad (27)$$

where a product of Clebsch–Gordan-coefficients appears on the rhs, and the electric field is expanded in the usual spherical basis with coefficients E_q, $q=-1,0,+1$. The optical potential couples different Zeeman sublevels if the field is not in a pure polarization state with respect to this basis. The matrix (27) then contains both diagonal and nondiagonal elements. The diagonal elements lead to the light-shift of the Zeeman sublevels, that are coupled by the nondiagonal elements.

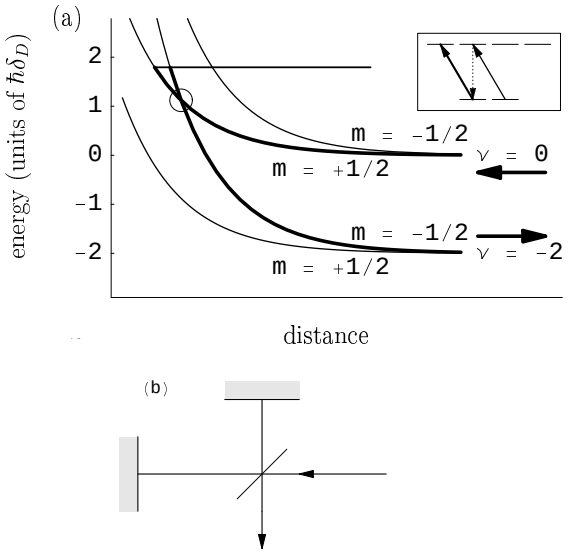

Fig. 7 (a) Potential energy surfaces for a $J=1/2\rightarrow J_e=3/2$ transition in a single (nearly) circularly polarized evanescent wave. The potentials cross where the difference between the light-shifts compensates for the Doppler shift. At this position, a linearly polarized copropagating wave leads to a resonant Raman coupling to the $\nu=-2$ diffraction channel (see inset). The kinetic energy $\frac{1}{2}mv_{zi}^2$ of the incident atoms is indicated by the thin horizontal line.
(b) Schematic representation of the diffraction process in terms of a Michelson interferometer. The level crossing of (a) is represented as a beamsplitter, and the turning points in the repulsive potentials as mirrors.

One may now proceed along similar lines as for the two-level theory, and compute the adiabatic potentials for the diffraction channels. These channels are labeled by the diffraction order $\nu=0,\pm2,\ldots$ and the magnetic sublevel m. Without a magnetic field and for fixed ν, the magnetic sublevels are asymptotically degenerate, while different diffraction orders ν are separated by twice the Doppler shift (at grazing incidence). An example is shown in Fig.7(a) for a $J_g=1/2$ ground state and a single running evanescent wave with TM polarization (magnetic field vector perpendicular to the optical plane of incidence). To a quite good approximation, this wave is in fact σ^- circularly polarized provided the laser beam is incident far beyond the critical angle. [The quantization axis is parallel to the magnetic field vector.] The degeneracy of the sublevels is lifted by the light field because the diagonal elements of the optical potential matrix (27) differ in magnitude for the sublevels $m=\pm1/2$ [see inset of Fig.7(a)]. As a consequence, the potentials for the diffraction orders $\nu=0,-2$ cross when the difference between the light shifts $\langle-1/2|\hat{V}(z)|-1/2\rangle$ and

$\langle +1/2|\hat{V}(z)|+1/2\rangle$ is larger than twice the Doppler shift. For a pure TM polarization, this is an exact crossing because there is no Raman coupling (the optical potential (27) has no off-diagonal elements). A coupling can be provided if one adds a second evanescent wave with linear (TE) polarization: starting from the sublevel $m = +1/2$, the atom absorbs a σ^- polarized photon from the strong counterpropagating (TM) wave and emits a stimulated photon with π polarization into the weak copropagating (TE) wave. The atom thus ends up in the $m = -1/2$ substate of the $\nu = -2$ diffraction channel [Fig.7(a), inset]. In the presence of the second evanescent wave, the adiabatic potentials form an avoided crossing at the position of the circle in Fig.7(a). There, an incoming wavefunction in the $|\nu = 0, m = +1/2\rangle$ channel is split in two parts that are subsequently reflected from their respective repulsive potentials and recombined after the second passage at the crossing. Note that for this particular model, the evanescent wave realizes a 'Michelson interferometer' with a single beamsplitter and two mirrors, as shown schematically in Fig.7(b).

4.3 Predictions

4.3.1 Numerical calculation. In Ref.[19], the Canberra theory group reported a numerical solution of the time-dependent Schrödinger equation for an atom with Zeeman-degenerate ground and excited states with $J_g = J_e = 2$. They studied a situation close to the experiment [8]: a diffraction grating formed by two evanescent waves and an unpolarized atomic beam (all magnetic sublevels equally populated). The population in the $\nu = -2$ diffraction channel is found of the order of 15 % if the optical polarization vectors are tilted (different combinations of TE and TM polarizations), in qualitative agreement with the experiment. Similar to the magnetic beam splitter [22], only a single Zeeman substate is involved in the multilevel diffraction mechanism. This suggests that a transfer efficiency close to 100 % could be possible with spin-polarized atoms.

4.3.2 Landau-Zener theory. In the following, we concentrate on analytical results obtained for the $J_g = 1/2$ ground state discussed above. The physical picture explained for this model can be translated into a simple theory when the avoided crossing is treated by means of the Landau-Zener model for nonadiabatic transitions [52]. Assuming that the atom moves through the crossing with a constant velocity (fixed by energy conservation), the Landau-Zener formula allows one to compute the probability amplitudes for the two potentials after the crossing. One thus obtains the reflection and transmission amplitudes for the beam splitter in Fig.7(b). Calculating the phase shifts between the beamsplitter and the turning points in the WKB approximation, we end up with the populations of the diffraction channels $|\nu = 0, m = +1/2\rangle$ and $|\nu = -2, m = -1/2\rangle$.

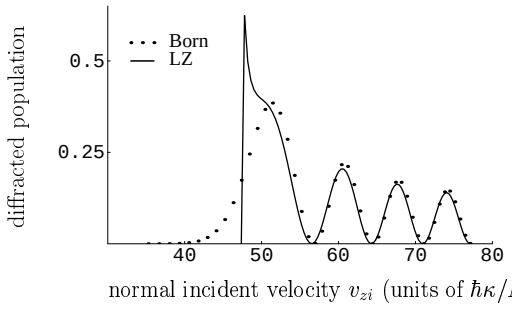

Fig. 8 (taken from Ref.[20]) Predictions of the Landau-Zener model (solid line) and the distorted-wave Born approximation (points) for the diffraction of a $J_g = 1/2$ atom from an evanescent wave diffraction grating with a weak polarization gradient. The diffracted population is shown as a function of the incident velocity component v_{zi} (in units of the 'recoil velocity' $\hbar\kappa/M$). The intensity $|\mathbf{E}_{TE}(z = 0)|^2$ of the TE polarized wave is equal to 6×10^{-4} the TM intensity.

The result of such a calculation is shown in Fig.8 (solid line), as a function of the incident velocity v_{zi} perpendicular to the grating. The incoming atom is in the substate $m = +1/2$, the diffracted atom being in $m = -1/2$. The diffracted population shows a maximum, and this happens if the position of the avoided crossing coincides with the atomic turning point. Since the atom then spends a long time in a region of resonant Raman coupling, this could have been expected.[5] For larger energies, the atomic wave explores both potential surfaces [cf. Fig.7(a)], and the diffraction populations show Stueckelberg oscillations due to the interference between the two paths. The diffracted population eventually decreases because the atomic velocity becomes larger and larger at the avoided crossing, reducing the splitting efficiency. The coincidence of the atomic turning point with the avoided crossing allows us to formulate the following condition for optimum diffraction:

$$\frac{\langle -1/2|\hat{V}(z_c)|-1/2\rangle}{\langle +1/2|\hat{V}(z_c)|+1/2\rangle} = \frac{E_{zi} + 2\hbar\delta_D}{E_{zi}} \qquad (28)$$

Due to the common exponential variation of the optical potentials, the lhs is in fact independent of z_c and only depends on the polarization of the evanescent field. Recalling that the atom must be reflected from both optical potentials, we recover the prediction of Deutschmann et al. [13] that a light-shift comparable to the Doppler shift is necessary for efficient diffraction.

[5] If the atomic velocity is precisely zero at the crossing, Landau-Zener predicts in fact that the atom adiabatically follows its initial potential surface, leading to zero diffraction. A very small deviation from this condition is sufficient, however, to produce a large transition probability and hence efficient diffraction.

4.3.3 Distorted-wave Born approximation. Although the Landau-Zener model indicates that diffraction is optimized if the atomic turning point coincides with the avoided crossing, this circumstance invalidates the model itself, because in the vicinity of the turning point one cannot describe the atom by a classical particle with a given velocity. We may however use an alternative approach based on the distorted-wave Born approximation. The Raman coupling is then treated as a perturbation that induces a coupling between the wavefunctions in the initial and final potentials. Note that these wavefunctions have asympotically different kinetic energies (in the normal direction) due to the Doppler effect. Analyzing the matrix element in Fermi's Golden Rule in analogy to the Franck–Condon factors familiar from molecular physics, we expect diffraction to be most efficient when the classical turning points of both wavefunctions coincide, since their amplitude is maximum there.[6] It is easy to see that this condition is in fact identical to (28). Fig.8 shows the result of the distorted-wave Born approximation (points). An optimum diffraction is indeed obtained close to the (unphysical) maximum of the Landau-Zener model (solid line), and both models are in good agreement for incident energies above the optimum.

4.4 Comparison to experiment

The numerical calculation [19] of the Canberra theory group is in fair agreement with the Bonn experiment [8], given the number of simplifications in the theory (evanescent wave of infinite size, omission of van der Waals interactions with the dielectric surface). For a more detailed comparison, experiments with spin-polarized atomic beams and well-controlled optical polarizations would be very useful. The theory indeed predicts a quite efficient population transfer (100 % do not seem excluded in principle), with promising applications for atomic interferometry.

We also note that experiments at large angle incidence may be 'simulated' in a normal incidence geometry, by introducing a frequency difference between the two counterpropagating evanescent waves, in a way similar to early diffraction experiments with bichromatic standing evanescent waves [6,7]. Experiments in this direction have been performed in the Orsay group and confirm the multilevel diffraction theory outlined above. For a quantitative comparison, however, the van der Waals interaction and, possibly, losses from spontaneous emission have to be taken into account. A detailed discussion will be published elsewhere.

[6] This picture yields still another interpretation of the grazing incidence cutoff in the one-level model: since the initial and final wavefunctions are subject to the same light shift, their turning points can only coincide if they have the same energy, which is impossible due to the Doppler effect. The Franck–Condon overlap is thus far from its maximum value.

5 Conclusion

The diffraction of neutral atoms from a stationary evanescent wave has remained, since its proposal in 1989, a fascinating challenge, both experimentally and theoretically. In the last decade, important breakthroughs have been achieved: detailed theoretical predictions for both grazing and normal incidence as well as successful experimental observations. Despite the conceptual simplicity of the setup, the diffraction mechanism turned out to be quite subtle. In close contact with the experimental efforts, theory has now evolved towards a picture where Raman transitions between magnetic sublevels of the atomic ground state play a crucial role. This feature endows atomic diffraction with a richer structure than, e.g., light diffraction [53], and it also allows one to construct tunable and nearly lossless atom-optical beamsplitters, using suitably polarized light fields far off resonance and/or magnetic fields. The field is still active and one observes an increased interest in specifically tailored light fields, using microfabricated surfaces [41,43], for grazing incidence reflection gratings. At normal incidence, it has become apparent that atoms moving in an evanescent wave provide a sensitive probe of van der Waals like surface interactions [23]. The combination with multilevel diffraction mechanisms suggests to probe this interaction with interferometric resolution and for well-defined Zeeman sublevels.

Another direction of current research may be termed 'coherent atom optics' where one studies the motion of a high-density (and ultimately Bose–Einstein condensed) atomic gas in laser fields. For instance, the evanescent wave mirror combined with gravity could be used to build an atomic resonator [54,55] where diffraction may serve as a convenient output coupler. At high densities in this resonator, one has to take into account the large refraction index of the trapped gas, modifying the evanescent wave [56]. A second example are atomic waveguides in hollow fibers: 'coating' the walls with an evanescent wave, efficient guiding has already been demonstrated [57–59]. Grazing incidence diffraction taught us that Raman couplings may mix the ground state sublevels and transfer large amounts of kinetic energy perpendicular to the wall. This problem will have to be faced on the route rowards single-mode atomic waveguides.

Acknowledgments

C. H. acknowledges support from the Ministère de la Recherche et de l'Enseignement Supérieur (France), from the Training and Mobility of Researchers Network 'Coherent Matter Wave Interactions' (European Union, contract ERBFMRX CT96-0002), and from the Deutsche Forschungsgemeinschaft (Germany, grant He 2849/1-1).

This work would have been impossible without fruitful discussions with many colleagues among whom we

would like to mention Rosa Brouri, Laurent Cognet, Jean-Yves Courtois, Jean Dalibard, Ralf Deutschmann, Gabriel Horvath, Robin Kaiser, Arnaud Landragin, Vincent Lorent, Klaus Mølmer, Tilman Pfau, and Andrew Steane.

References

1. R. J. Cook, R. K. Hill: Opt. Commun. **43**, 258 (1982)
2. J. V. Hajnal, G. I. Opat: Opt. Commun. **71**, 119 (1989)
3. C. Adams, M. Siegel, J. Mlynek: Phys. Rep. **240**, 143 (1994)
4. H. Wallis: Phys. Rep. **255**, 203 (1995)
5. Adv. At. Mol. Opt. Phys., edited by P. R. Berman. New York: Academic Press 1997, Vol. 37, Suppl. 3
6. J. V. Hajnal, K. G. H. Baldwin, P. T. H. Fisk, H.-A. Bachor, G. I. Opat: Opt. Commun. **73**, 331 (1989)
7. B. W. Stenlake, I. C. M. Littler, H.-A. Bachor, K. G. H. Baldwin, P. T. H. Fisk: Phys. Rev. A **49**, R16 (1994)
8. M. Christ, A. Scholz, M. Schiffer, R. Deutschmann, W. Ertmer: Opt. Commun. **107**, 211 (1994)
9. R. Brouri, R. Asimov, M. Gorlicki, S. Feron, J. Reinhardt, V. Lorent, H. Haberland: Opt. Commun. **124**, 448 (1996)
10. A. Landragin, L. Cognet, G. Z. K. Horvath, C. I. Westbrook, N. Westbrook, A. Aspect: Europhys. Lett. **39**, 485 (1997)
11. A. Steane, P. Szriftgiser, P. Desbiolles, J. Dalibard: Phys. Rev. Lett. **74**, 4972 (1995)
12. A. Landragin, G. Labeyrie, C. Henkel, R. Kaiser, N. Vansteenkiste, C. I. Westbrook, A. Aspect: Opt. Lett. **21**, 1581 (1996)
13. R. Deutschmann, W. Ertmer, H. Wallis: Phys. Rev. A **47**, 2169 (1993)
14. J. E. Murphy, P. Goodman, A. E. Smith: J. Phys.: Condens. Matter **5**, 4665 (1993)
15. J. E. Murphy, L. C. L. Hollenberg, A. E. Smith: Phys. Rev. A **49**, 3100 (1994)
16. C. M. Savage, D. Gordon, T. C. Ralph: Phys. Rev. A **52**, 4741 (1995)
17. C. Henkel, J.-Y. Courtois, A. Aspect: J. Phys. II (France) **4**, 1955 (1994)
18. P. Storey, C. Cohen-Tannoudji: J. Phys. II (France) **4**, 1999 (1994)
19. D. Gordon, C. M. Savage: Opt. Commun. **130**, 34 (1996), **136**, 503(E) (1997). [Complete corrected version: atom-ph/9404004]
20. C. Henkel, K. Mølmer, R. Kaiser, C. I. Westbrook: Phys. Rev. A **56**, R9 (1997)
21. R. Deutschmann, Ph.D. thesis, Universität Hannover, 1997, unpublished
22. R. Deutschmann, W. Ertmer, H. Wallis: Phys. Rev. A **48**, R4023 (1993)
23. A. Landragin, J.-Y. Courtois, G. Labeyrie, N. Vansteenkiste, C. I. Westbrook, A. Aspect: Phys. Rev. Lett. **77**, 1464 (1996)
24. R. Côté, H. Friedrich, J. Trost: Phys. Rev. A **56**, 1781 (1997)
25. A. F. Devonshire: Proc. Roy. Soc. London, Ser. A **156**, 37 (1936)
26. J. M. Jackson, N. F. Mott: Proc. Roy. Soc. (London) Ser. A **137**, 703 (1932)
27. C. Henkel, J.-Y. Courtois, R. Kaiser, C. I. Westbrook, A. Aspect: Laser Physics **4**, 1040 (1994)
28. G. Armand, J. R. Manson: Phys. Rev. Lett. **43**, 1839 (1979)
29. C. Henkel, A. M. Steane, R. Kaiser, J. Dalibard: J. Phys. II (France) **4**, 1877 (1994)
30. W. A. Steele: Surf. Sci. **97**, 478 (1980)
31. D. V. Kulginov, N. V. Blinov: Surf. Sci. **313**, 120 (1994)
32. P. J. Martin, B. G. Oldaker, A. H. Miklich, D. E. Pritchard: Phys. Rev. Lett. **60**, 515 (1988)
33. C. Henkel, C. I. Westbrook, A. Aspect: J. Opt. Soc. Am. B **13**, 233 (1996)
34. B. Segev, R. Côté, M. G. Raizen: Phys. Rev. A **56**, R3350 (1997)
35. M. Born, E. Wolf: *Principles of Optics*. London: Pergamon Press 1959
36. A. C. Levi, H. Suhl: Surf. Sci. **88**, 221 (1979)
37. G. I. Opat, S. J. Wark, A. Cimmino: Appl. Phys. B **54**, 396 (1992)
38. J. Felber, R. Gähler, C. Rausch, R. Golub: Phys. Rev. A **53**, 319 (1996)
39. C. J. Bordé: in Adv. At. Mol. Opt. Phys., edited by P. R. Berman. New York: Academic Press 1997, Vol. 37, Suppl. 3
40. P. J. Martin, P. L. Gould, B. G. Oldaker, A. H. Miklich, D. E. Pritchard: Phys. Rev. A **36**, R2495 (1987)
41. V. I. Balykin, D. A. Lapshin, M. V. Subbotin, V. S. Letokhov: Opt. Commun. **145**, 322 (1998)
42. L. Cognet, V. Savalli, G. Zs. K. Horvath, N. Westbrook, C. I. Westbrook, A. Aspect: to be submitted (1998)
43. A. Roberts, J. E. Murphy: Opt. Commun. **128**, 41 (1996)
44. N. S. Witte: J. Phys. A **31**, 807 (1998)
45. J. Dalibard, C. Cohen-Tannoudji: J. Opt. Soc. Am. B **2**, 1707 (1985)
46. E. Kyrölä, S. Stenholm: Opt. Commun. **22**, 123 (1977)
47. C. Henkel, Ph.D. thesis, Université de Paris-Sud (Orsay), 1996, unpublished
48. A. P. Kazantsev, G. I. Surdovitch, V. P. Yakovlev: Pis'ma Zh. Eksp. Teor. Fiz. **31**, 542 (1980) [JETP Lett. **31**, 509–512 (1980)]
49. S. Feron et al.: Phys. Rev. A **49**, 4733 (1994)
50. M. Marte, S. Stenholm: Appl. Phys. B **54**, 443 (1992)
51. E. Schumacher, M. Wilkens, P. Meystre, S. Glasgow: Appl. Phys. B **54**, 451 (1992)
52. C. Zener: Proc. Roy. Soc., Ser. A **137**, 696 (1932)
53. Light diffraction from objects with polarization gradients is discussed in J. M. C. Jonathan: Opt. Commun. **40**, 239 (1981); T. Huang, K. H. Wagner: J. Opt. Soc. Am. B **13**, 282 (1996)
54. H. Wallis, J. Dalibard, C. Cohen-Tannoudji: Appl. Phys. B **54**, 407 (1992)
55. H. Wallis: J.E.O.S. B: Quantum Semiclass. Opt. **8**, 727 (1996)
56. H. Wallis: Phys. Rev. A **56**, 2060 (1997)
57. M. J. Renn, E. A. Donley, E. A. Cornell, C. E. Wieman, D. Z. Anderson: Phys. Rev. A **53**, R648 (1996)
58. H. Ito, T. Nakata, K. Sakaki, M. Ohtsu, K. I. Lee, W. Jhe: Phys. Rev. Lett. **76**, 4500 (1996)
59. G. Wokurka, J. Keupp, K. Sengstock, W. Ertmer: to be submitted (1998); and communication Q 43.1 at the spring meeting of the German Physical Society (Konstanz, march 1998): Verhandl. DPG (VI) **33**, 207 (1998)